The pore-scale distribution of sediment-hosted hydrates: evidence from effective medium modelling of laboratory and borehole seismic data

T. A. Minshull[1] and S. Chand[2]

[1] National Oceanography Centre, European Way, Southampton SO14 3ZH, UK; tmin@noc.soton.ac.uk

[2] Geological Survey of Norway (NGU), Tromsøkontoret, Polarmijløsenteret, 9296, Tromsø, Norway; shyam.chand@ngu.no

Abstract

Much of our knowledge of hydrate distribution in the subsurface comes from interpretations of remote seismic measurements. A key step in such interpretations is an effective medium theory that relates the seismic properties of a given sediment to its hydrate content. A variety of such theories have been developed; these theories generally give similar results if the same assumptions are made about the extent to which hydrate contributes to the load-bearing sediment frame. We have further developed and modified one such theory, the self-consistent approximation/differential effective medium approach, to incorporate additional empirical parameters describing the extent to which both the sediment matrix material (clay or quartz) and the hydrate are load-bearing. We find that a single choice of these parameters allows us to match well both P and S wave velocity measurements from both laboratory and *in situ* datasets, and that the inferred proportion of hydrate that is load-bearing varies approximately linearly with hydrate saturation. This proportion appears to decrease with increasing hydrate saturation for gas-rich laboratory environments, but increase with hydrate saturation when hydrate is formed from solution and for an *in situ* example.

Introduction

In order to assess the significance of gas hydrate as a resource, as a hazard, and as an agent in climate change, it is necessary to determine how much hydrate is present in subsurface sediments. The most reliable measure of hydrate saturation comes where there is direct sampling and core material is recovered under pressure; hydrate

saturations may then be estimated accurately from the volume of methane evolved during decompression (e.g., Dickens et al., 1997). Such direct sampling provides essential "ground truth" for geophysical estimates of hydrate saturation, but is expensive and can only be carried out in a very few locations that may not be representative. Therefore, for most of our information on hydrate volumes we must rely on remote geophysical methods. The replacement of conductive (normally saline) pore water with resistive hydrate in the pore space can lead to significant anomalies in electrical resistivity, and some progress has been made in the measurement of such anomalies (e.g., Schwalenberg et al., 2005). In principle, hydrate saturations may also be estimated using sensitive measurements of the response of the seafloor to tidal variations in seafloor pressure (Latychev & Edwards, 2003). However, seismic techniques remain the primary remote methods used to determine hydrate content of the subsurface. With an appropriately designed experiment, detailed knowledge may be obtained of P and S wave velocities within the hydrate stability zone (e.g., Singh et al., 1993; Hobro et al., 2005; Westbrook et al., 2005).

A key step in the process of remotely determining hydrate content is a quantitative relationship between that content and the physical properties measured, namely seismic velocities. The elastic properties of the individual components of hydrate-bearing sedimentary rocks (water, hydrate, quartz, clay minerals, etc) are generally well known, though those of clay minerals are difficult to measure and normally must be determined indirectly (e.g., Hornby et al., 1994). Methods that combine these component properties into the properties of the composite material are called "effective medium theories", and a key factor in the predictions of such theories is the extent to which hydrate is assumed to contribute to the strength of the sediment frame. In this paper we discuss briefly the advantages and limitations of such theories and then focus on the application of one particular theoretical approach to a range of datasets where the hydrate content is known from independent observations. The approach is described in more detail by Chand et al. (2006). Here we summarise the results of Chand et al. (2006) and further develop some of their ideas.

Effective Medium Theories

The most widely used effective medium theories were reviewed and compared by Chand et al. (2004). The simplest of such theories are essentially empirical correlations, such as the "weighted equation" approach applied to hydrate-bearing sediments by Lee et al. (1996). An advantage of this approach is that it can be readily adjusted to match any dataset, but because it has no physical basis, its application leads to little understanding of the physics involved and it is difficult to apply to areas away from or sediment types distinct from those in which the correlations have been developed. Therefore many authors prefer more sophisticated approaches that have some physical basis. Ideally such rock physics based approaches would have no adjustable parameters other than the unknown hydrate content. However, in the case of real sedimentary rocks, even if parameters such as composition and porosity are perfectly known, assumptions must be made about the way the different components are organised and generally these assumptions must be modified in some way to fit real data – hence these approaches retain empirical elements.

The rock physics based approaches reviewed by Chand et al. (2004) include the self-consistent approximation/differential effective medium (SCA/DEM) approach of Jakobsen et al. (2000), the three-phase effective medium model (TPEM) of Ecker et al. (1998) and Helgerud et al. (1999), and the three-phase Biot theory (TPB) developed by Gei and Carcione (2003). Each of these approaches involves different simplifying assumptions regarding the shapes of individual sediment components and the way in which they interact with each other. All assume that, on the scale of a seismic wavelength, there is a degree of uniformity in the hydrate distribution, and that hydrate is disseminated in some way through the pore space. Hence none of these approaches copes well if hydrate occurs dominantly in nodules or veins, a form that may be important in some fine-grained sediments (e.g., Holland et al., 2006).

Jakobsen et al. (2000) developed two versions of the SCA/DEM approach: one in which the SCA is applied initially to a clay-water mixture, to simulate a microstructure in which hydrate is formed inside pores and is not load-bearing, and a second in which the SCA is applied initially to a clay-hydrate mixture, to simulate a microstructure in which the hydrate forms at pore throats and is load-bearing. Here

we use the term "clay" to indicate clay minerals, rather than as a grain-size descriptor. Similarly, Helgerud et al. (1999) describe two versions of the TPEM approach: one in which hydrate forms part of the pore fluid and one in which hydrate forms part of the sediment frame.

Because of the difficulty of recovering and performing experiments on hydrate-bearing sediments without causing hydrate dissociation, direct observations of the pore-scale distribution of hydrates under *in situ* conditions are sparse. Sophisticated techniques such as thermal imaging have been developed to determine the hydrate distribution within pressurized cores (Weinberger et al., 2005; Expedition 311 Scientists, 2005), but such techniques do not resolve down to the scale of individual pores. Tohidi et al. (2001) showed that hydrate grown from solution on a two-dimensional glass substrate formed preferentially in the centres of pores, but the extent to which this idealised environment simulates nature is unclear.

As discussed in more detail by Chand et al. (2004), the models that assume hydrate forms part of the pore fluid result in similar predictions of P and S wave velocity as a function of hydrate saturation (Fig. 1). Similarly, models that assume that the hydrate is load-bearing make result in similar predictions (Fig. 2), but for most hydrate saturations the predicted velocities are significantly higher than those of any of the models in which hydrate forms part of the pore fluid. The two models of Helgerud et al. (1999) converge with each other at low hydrate saturations and diverge at high saturations. Conversely, the two models of Jakobsen et al. (2000) converge at high saturations and diverge at low saturations, so that they predict different results when no hydrate is present – a clearly unphysical result. This result led Chand et al. (2006) to develop a modification to Jakobsen et al.'s basic approach in which hydrate is split into two component parts. For clay-rich sediments, a clay-water starting model is used throughout and the part of the hydrate that is not load-bearing is treated as inclusions (rather than replacing water in the clay-water starting model), while the part that is load-bearing replaces clay so that it properly forms part of the sediment frame. The velocities predicted by this modified approach, for the end member cases of all and none of the hydrate being load-bearing, converge at low hydrate saturations and diverge at high saturations (Fig. 3). This is physically more realistic result that is also compatible with results from the model of Helgerud et al. (1999).

Effective Medium Inversion

The models described above can be turned around to infer hydrate saturations from observed seismic velocities, provided that other key parameters (porosity, composition, and the elastic properties of the components) are known. A formal inverse approach to this problem was developed by Chand et al. (2006). The inversion is able to use measurements of P and S wave velocity, and also, if available, P and S wave attenuation. Formal uncertainties are also estimated, though these take into account only the uncertainties in the input parameters; it is difficult to account for the uncertainties in the effective medium models themselves.

Figure 4 illustrates the results of applying such an approach to a dataset from offshore Vancouver Island (Hobro et al., 2005). In this case there is information on porosity and lithology from Ocean Drillling Program Site 889, which lies within the survey area; the inversion used an exponential decay of porosity with depth and a mean sediment composition based on data from this site. Velocity information comes from a low-resolution P-wave tomographic study. The resolution of such studies is clearly an issue in this area and probably in most hydrate provinces: recent work in the same area during Integrated Ocean Drilling Program Expedition 311 (Riedel et al., 2006) has revealed a highly heterogeneous hydrate distribution. The tomographic model smooths the velocities over length scales of several hundred metres horizontally and several tens of metres vertically (Hobro et al., 2005). Unfortunately, the relationship between hydrate saturation and velocity is not linear (Figs 1-3), so even if the effective medium model is perfectly accurate, applying the effective medium inversion to a mean velocity over a given volume does not necessarily yield an accurate value for the hydrate content of that volume. However, a much larger uncertainty comes from the effective medium models themselves. While the model used by Hobro et al. (2005) yields a maximum hydrate saturation of c. 15%, other models predict saturations up to double this value (Fig. 4). Using the model of Chand et al. (2006) with the proportion of hydrate that is load-bearing set equal to the hydrate saturation, inferred saturations are c. 50% higher than those of Hobro et al. (2005), because at low hydrate saturations, the velocities predicted by this model are significantly lower (Fig. 3). This calculation is purely illustrative: such a relationship

between hydrate saturation and hydrate cementation is based loosely on some calibration data that is described below, and may not be valid for the Vancouver Island margin.

The proportion of hydrate that is assumed to be load-bearing is effectively a free parameter in the SCA/DEM model, since it is impossible *a priori* to calculate what its value should be in a given geological environment. Therefore to choose sensibly between the results shown in Fig. 4, some calibration data are required for which the hydrate content is known independently. In the next two sections we examine some datasets from both laboratory and field studies that might be used for calibration. An unavoidable limitation of such calibration datasets is that they involve higher seismic frequencies and correspondingly smaller sampling volumes than the field datasets that we wish to interpret. This limitation does not compromise the calibration if heterogeneities are smaller than the seismic wavelength of the calibration data.

Application to Laboratory Data

Our first calibration dataset is the dataset of Priest et al. (2005). These authors prepared methane hydrate bearing sand samples by melting fine-grained ice particles in the presence of methane gas, following the method of Stern et al. (1996). Velocities were measured at seismic frequencies using a resonant column with both torsional and flexural vibrations, to determine P and S wave velocities respectively. Hydrate saturations were controlled by controlling the amount of ice/water in the system and were therefore accurately known. The resulting hydrate-bearing sediment is essentially dry; absence of residual water was confirmed by freezing the samples and checking that there was no significant change in velocities (Priest et al., 2005).

Unfortunately, application of the SCA/DEM approach to a quartz-air mixture leads to computed velocities that are much higher than those observed. In order to match these data, Chand et al. (2006) further modified the SCA/DEM approach. Instead of incorporating all of the quartz in the bi-connected SCA/DEM model, only a small proportion of the quartz is included at this stage, and the remainder is incorporated as isolated inclusions. Much lower velocities can then be obtained (Fig. 5). Both P and S wave observations may be matched if between 1% and 5% of the quartz is load-

bearing (1-5% cementation). Such low percentages are reasonable given the way the samples are made. The percentage increases with differential pressure, which is physically reasonable as areas of grain contact will increase with increasing pressure. This approach gives us a second empirical factor (the degree of cementation of the host matrix) that is required to match real observations.

Having achieved a fit to the data in the absence of hydrate, the observations with hydrate present may than be matched by varying the degree of hydrate cementation as described in the previous section. At very low hydrate saturations, the predicted velocity is insensitive to the degree of cementation. However at hydrate saturations of a few percent, all of the hydrate must be cementing (as concluded also by Priest et al., 2005), while at higher saturations, the degree of hydrate cementation required drops to about 40% (Fig. 6). The fact that, for both empirical parameters, the same value fits both P and S wave velocities, indicates that the approach taken is not a bad approximation to the physics involved.

Application to Borehole Data

The above laboratory work uses a sediment type (pure sand) that is not normally present in hydrate provinces in nature, and the hydrate is made in a way that does not approximate natural processes of hydrate formation. Therefore the insights obtained regarding the variation of cementation with saturation may have limited applicability. Calibration of the effective medium approach with a real field dataset, for which the hydrate content is known, is therefore desirable. Unfortunately, knowledge of *in situ* hydrate contents requires direct sampling, at pressure, by drilling, and few such datasets are available. However, in several hydrate provinces, estimates of hydrate saturation are available based on borehole resistivity data. Hydrate saturations are commonly derived from such data using Archie's law, an empirical effective medium approach which appears to give reliable estimates of the pore fluid component in a wide range of geological settings. These estimates must be treated with caution because of their empirical origin, but they are at least independent of seismic measurements.

One such dataset that has been widely used is from the Mallik 2L-38 borehole in the Canadian Arctic (Collett et al., 1999). A limitation of this dataset for calibration purposes is that porosities are significantly lower than those at equivalent depths in deep marine environments and the clay content is relatively low. Based on resistivity, hydrate saturations reach 80% at some depths in the hole, and both P and S wave velocities are available from borehole logs. In the absence of hydrate, velocities are around 2.2 km/s at a porosity of around 38%. These velocities are much higher than those of the hydrate-free laboratory sand samples described above (Fig. 5), which have slightly higher porosity, and also much higher than those of Yun et al.'s (2005) sand samples at a similar porosity (37%). Velocities are higher despite the fact that the Mallik material contains about 50% clay minerals, which have lower elastic moduli than quartz. This difference illustrates the importance of cementation: at Mallik the matrix material (clay) is much more strongly connected than the laboratory quartz samples, and in our approach is modelled as 100% load-bearing, in contrast to the 1-5% connected laboratory sand sample described above. The effect of hydrate cementation on velocity is much less in such circumstances than in the case of the laboratory samples.

When plotted as a function of hydrate saturation, P and S wave velocities are quite scattered (Fig. 7) because they depend also on porosity and composition, which vary through the interval sampled. In general, this scatter is larger than the variation of predicted velocities with degree of cementation for fixed porosity and clay content, though at high hydrate saturations there is some indication that a better fit is achieved to both P and S wave velocities if the degree of hydrate cementation is high, in contrast to the low degrees of cementation required for the laboratory data described above. This effect may be seen much more clearly if the degree of hydrate cementation required to match the observations is displayed as a function of hydrate saturation (Fig. 8), since then variations in porosity and composition may be accounted for directly. Degrees of hydrate cementation inferred from S wave velocities differ little from those inferred from P wave velocities, again suggesting that we are achieving a reasonable approximation to the physics involved.

Other datasets may be represented in the same way. We have also modelled the results of Waite et al. (2004), who measured ultrasonic P wave velocities on hydrate-

bearing samples of partially water-saturated sands. Hydrate was made in these samples by passing gas through the samples at high pressure. As with the resonant column results of Priest et al. (2005), these data are matched by a systematic decrease of hydrate cementation with saturation (Fig. 8), though the decrease is not as steep as for the dry samples of Priest et al. Finally, we applied our method to measurements of P and S wave velocities made by Yun et al. (2005) on hydrate-bearing sand samples made using tetrahydrofuran in solution. In contrast to the other laboratory datasets, these data are matched by very low degrees of hydrate cementation, and the inferred degree of cementation increases systematically with hydrate saturation (Fig. 8).

Discussion

As with all effective medium methods, the SCA/DEM method requires some empirical adjustments to fit real data. The advantage of the approach we describe above is that the adjustments can be related to something physical – the extent to which different components are load-bearing or "cementing". Using a variety of published datasets, and assuming that the effect that we model as cementation is indeed cementation, we can determine how cementation varies with hydrate saturation based on independent determinations of the latter. Results are consistent whether we use P or S wave velocities, and the inferred variations of cementation with hydrate content are systematic and approximately linear. Unfortunately, the slopes of the trends in Figure 8 vary in both magnitude and sign depending on how the hydrate has been formed. For samples made in a gas-rich environment. where hydrate may tend to form initially at grain contacts (Priest et al., 2005), the inferred hydrate cementation decreases with saturation. For samples formed from solution, the inferred hydrate cementation increases with saturation. For the *in situ* data from Mallik 2L-38, the inferred cementation increases with saturation, but more steeply than for the laboratory samples formed from solution.

In many field situations, an analysis of the type described above will not be possible, because remote seismic observations form the only constraint available on hydrate saturations. In such situations, the following approach may be taken:

1. Define a no-hydrate reference velocity curve based on velocities in regions where no hydrate is thought to be present (e.g., close to the seabed and/or beneath the base of the hydrate stability field), and use this curve and estimates of porosity to determine how the proportion of sediment grains that are load-bearing varies with porosity. This step will be more robust if both P and S wave velocity measurements are available.
2. Generate an empirical, linear or at least monotonic, fit between inferred hydrate cementation and hydrate saturation either using borehole data from the same area (if there is a borehole sampling hydrate), or from similar hydrate-bearing sediments elsewhere.
3. Assume that this empirical fit applies throughout the volume sampled by seismic data and hence infer hydrate saturations.

The above approach is limited by the several assumptions that are required, including the assumption that the hydrate is uniformly disseminated in the pore space and that within the pore space it takes one of the forms described by the DEM theory. Given these assumptions, the main potential for error comes from the second step. A way forward is to develop a larger database of *in situ* seismic velocity measurements where hydrate saturations are known independently. Such a database is gradually emerging through scientific ocean drilling (Trehu et al., 2004; Expedition 311 Scientists, 2005).

An alternative, more direct approach may be to further develop geophysical techniques that remotely determine other sediment physical properties such as electrical resistivity. The resistivity of hydrate-bearing sediments will depend also on the way the different components are connected, and in particular the connectivity of the fluid component. Simultaneous remote measurement of both seismic and electrical properties would yield an additional constraint that may remove some of the ambiguities that come from the use of seismic data alone. Interpretation of such datasets will require a joint effective medium approach that can model both seismic velocity and resistivity (Ellis et al., 2005).

Conclusions

From our effective medium calculations and their calibration through laboratory and borehole measurements, we conclude the following:

1. The prediced physical properties of hydrate-bearing sediments depend more strongly on the assumed microstructure than on the particular effective medium model used to approximate them.
2. Both laboratory and borehole measurements of the seismic velocity of hydrate-bearing sediments may be modelled successfully using a modified version of the SCA/DEM approach.
3. For laboratory samples made in the presence of excess gas, the proportion of hydrate that is load-bearing appears to decrease with increasing hydrate saturation.
4. For borehole data from the Canadian Arctic, and for laboratory samples made from solution, this proportion appears to increase with increasing hydrate saturation.
5. Such systematic variations ultimately might be used to infer more accurately hydrate saturations from remote seismic data.

Acknowledgments

The early part of this work was supported by the European Commission under the contract EVK3-CT-2000-00043 (HYDRATECH). We thank J. Priest, A. Best and W. Waite for access to data and for useful discussions, and P. Jackson and an anonymous reviewer for constructive comments.

References

Chand, S., Minshull, T.A., Gei, D. & Carcione, J.M., 2004. Elastic velocity models for gas-hydrate bearing sediments – A comparison, *Geophysical Journal International,* 159, 573-590.

Chand, S., Minshull, T. A., Priest, J. A., Best, A. I., Clayton, C. R. I., Waite, W. F. 2006. An effective medium inversion algorithm for gas hydrate quantification and its application to laboratory and borehole measurements of gas hydrate bearing sediments, *Geophysical Journal International*, in press.

Collett, T.A., Lewis, R.E., Dallimore, S.R., Lee, M.W., Mroz, T.H. & Uchida, T., 1999. Detailed evaluation of gas hydrate reservoir properties using JAPEX/JNOC/GSC Mallik 2L-38 gas hydrate research well down hole well-log displays, in Scientific Results from JAPEX/JNOC/GSC Mallik 2L-38 Gas Hydrate Research Well, Mackenzie Delta, Northwest Territories, Canada, Geological Survey of Canada Bulletin 544, pp. 295-312, eds. Dallimore, S.R., Uchida, T., & Collet, T.S., Geological Survey of Canada, Ottawa, Canada.

Dickens, G. R., Paull, C. K. & Wallace, P. 1997. Direct measurement of in situ methane quantities in a large gas-hydrate reservoir, *Nature*, 385, 428-428.

Ecker, C., Dvorkin, J. & Nur, A. 1998. Sediments with gas hydrates: Internal structure from seismic AVO, *Geophysics*, 63, 1659-1669.

Ellis, M. H., T. A. Minshull, A. I. Best, M. C. Sinha & J. Sothcott, 2005. Joint seismic and electrical measurements of gas hydrates in continental margin sediments, *Proc. 5th Int. Conf. on Natural Gas Hydrates*, 2, paper 2022, 545-554.

Expedition 311 Scientists, 2005. Cascadia margin gas hydrates, *IODP Prel. Rept*, 311, doi:10.2204/iodp.pr.311.2005.

Gei, D. & Carcione, J.M., 2003. Acoustic properties of sediments saturated with gas hydrate, free gas and water, *Geophysical Prospecting,* 51, 141-157.

Helgerud, M. B., Dvorkin, J., Nur, A., Sakai, A. & Collett, T. 1999. Elastic-wave velocity in marine sediments with gas hydrates – Effective medium modeling. *Geophys. Res. Lett.*, 26, 2021-2024.

Hobro, J. W. D., Minshull, T. A., Singh, S. C. & Chand, S. 2005. A three-dimensional seismic tomographic study of the gas hydrate stability field, offshore Vancouver Island, *J. Geophys. Res*., 110, B09102, doi:10.1029/2004JB003477.

Holland, M., Schultheiss, P., Roberts, J., Druce, M., IODP Expedition 311 Shipboard Scientific Party & NGHP Expedition 1 Shipboard Scientific Party 2006. Hydrate-sediment morphologies revealed by pressure core analysis, *Eos, Trans. Am. Geophys. Union, Fall Meeting Supplement,* OS33B-1689.

Hornby, B.E., Schwartz, L.M. & Hudson, J.A., 1994. Anisotropic effective-medium modelling of the elastic properties of shales*, Geophysics*, 59, 1570-1581.

Jakobsen, M., Hudson, J.A., Minshull, T.A. & Singh, S.C., 2000. Elastic properties of hydrate-bearing sediments using effective medium theory, *Jour. Geophys. Res.*, 105, 561-577.

Latychev, K. & Edwards, R. N. 2003. On the compliance method and the assessment of three-dimensional seafloor gas hydrate deposits, *Geophys. J. Int.*, 155, 923-952.

Lee, M.W., Hutchinson, D.R., Collett, T.S. & Dillon, W.P., 1996. Seismic velocities for hydrate-bearing sediments using weighted equation, *Jour. Geophys. Res.*, 101, 20347-20358.

Priest, J.A., Best, A.I. & Clayton, C.R.I., 2005. A laboratory investigation into the seismic velocities of methane gas hydrate-bearing sand, *Journal of Geophysical Research-Solid Earth*, 110, B04102, doi:10.1029/2004JB003259.

Schwalenberg, K., Willoughby E., Mir, R. & Edwards, R. N. 2005. Marine gas hydrate electromagnetic signatures in Cascadia and their correlation with seismic blank zones. *First Break*, 23, 57-63.

Singh, S.C., Minshull, T.A. & Spence, G.D., 1993. Velocity structure of a gas hydrate reflector, *Science*, 260, 204-207.

Stern, L.A., Kirby, S.H. & Durham, W.B., 1996. Peculiarities of methane clathrate hydrate formation and solid state deformation, including possible super heating of water ice, *Science*, 273, 10299-10311.

Tohidi, B., Anderson, R., Clennell, M. B., Burgass, R. W. & Biderkab, A. B. 2001. Visual observation of gas-hydrate formation and dissociation in synthetic porous material by means of glass macromodels, *Geology*, 29, 867-870.

Trehu, A.M., Long P.E., Torres M.E., Bohrmann G., Rack F.R., Collett T.S., Goldberg D.S., Milkov A.V., Riedel M., Schultheiss P., Bangs N.L., Barr S.R., Borowski W.S., Claypool G.E., Delwiche M.E., Dickens G.R., Gracia E., Guerin G., Holland M., Johnson J.E., Lee Y.J., Liu C.S., Su X., Teichert B., Tomaru H., Vanneste M., Watanabe M., & Weinberger J.L. 2004. Three-dimensional

distribution of gas hydrate beneath southern Hydrate Ridge: constraints from ODP Leg 204, *Earth Planet. Sci. Lett.*, 222, 845-862.

Waite, W.F., Winters, W.J. & Mason, D.H., 2004. Methane hydrate formation in partially water-saturated Ottawa sand, *American Mineralogist*, 89, 1202-1207.

Weinberger, J. L., Brown, K. M., & Long, P. E., 2005. Painting a picture of gas hydrate distribution with thermal images, *Geophysical Research Letters*, 32, L04609, doi:10.1029/2004GL021437.

Westbrook, G. K., S. Buenz, A. Camerlenghi, J. Carcione, S. Chand, S. Dean, J.-P. Foucher, E. Flueh, D. Gei, R. Haacke, F. Klingelhoefer, C. Long, G. Madrussani, J. Mienert, T. A. Minshull, H. Nouzé, S. Peacock, G. Rossi, E. Roux, T. Reston, M. Vanneste & M. Zillmer, 2005. Measurement of P- and S-wave velocities, and the estimation of hydrate concentration at sites in the continental margin of Svalbard and the Storegga region of Norway, *Proc. 5th Int. Conf. on Natural Gas Hydrates*, *3*, paper 3004, 726-735.

Yun, T.S., Francisca, F.M., Santamarina, J.C. & Ruppel, C., 2005. Compressional and shear wave velocities in uncemented sediment containing gas hydrate, *Geophysical Research Letters*, 32, L10609, doi:10.1029/2005GL022607.

Figure Captions

Figure 1. Variation of P wave (larger values) and S wave velocities with hydrate saturation at fixed porosity (50%) and clay content (50%), for the four models discussed by Chand et al. (2004); other parameters required by the models are given by Chand et al. (2004). Thick solid line corresponds to the SCA/DEM model of Jakobsen et al. (2000) with a clay-water starting model. Thin solid line corresponds to the TPEM model of Helgerud et al. (1999) with hydrate forming part of the pore fluid. Dashed line corresponds to the TPB model of Gei & Carcione (2003). Dotted line corresponds to the weighted equation of Lee et al. (1996).

Figure 2. Variation of P and S wave velocity with hydrate content for same materials as in Fig. 1, but for models in which hydrate forms part of the sediment frame. Thick line corresponds to the SCA/DEM model with a clay-hydrate starting model. Thin line corresponds to the load-bearing hydrate model of Helgerud et al. (1999). Grey area marks the range of predictions from the rock physics based models (i.e., excluding the weighted equation) of Fig. 1.

Figure 3: Results from applying the SCA/DEM approach of Jakobsen et al. (2000) in several different ways to a real continental margin sediment. Sediment properties are those described by Hobro et al. (2005). Upper set of curves correspond to P wave velocities and lower set of curves correspond to S wave velocities. Thin solid lines mark results from using clay-water (lower curves) and clay-hydrate (upper curves) starting model. Dotted curves mark results from the model used by Hobro et al. (2005) in which the clay-water and clay-hydrate models are linearly mixed. Other lines mark results from the "variable cementation" approach of Chand et al. (2006). Thick solid lines mark results from assuming that the hydrate is 0% (lower curves) and 100% (upper curves) load-bearing. Dashed line marks result from assuming that the proportion of hydrate that is load-bearing is equal to the hydrate saturation.

Figure 4. Estimates of hydrate saturation at the base of the hydrate stability field from the tomographic velocity model of Hobro et al. (2005): a) using the approach of Chand et al. (2006) and assuming that none of the hydrate is load-bearing; b) using the approach of Chand et al. (2006) and assuming that all of the hydrate is load-

bearing; c) using the approach of Hobro et al. (2005); d) using the approach of Chand et al. (2006) and assuming that the proportion of hydrate that is load-bearing is equal to the hydrate saturation.

Figure 5. a) Squares mark P wave velocities derived from resonant column measurements by Priest et al. (2005) for loose sand, and circles for tight sand. The higher velocities correspond to higher effective pressures. Curves mark predictions of modified SCA/DEM model for a quartz-air mixture, labelled with the proportion of quartz that is considered load-bearing (see text). b) Same as a) but for S wave velocities.

Figure 6. Triangles with error bars mark velocities derived from resonant column measurements by Priest et al. (2005). Curves mark predictions of the modified SCA/DEM model and are labelled with the degree of hydrate cementation, for sand with a porosity of 42.1%, which is the mean porosity of the laboratory samples: a) P wave velocities; b) S wave velocities (modified from Chand et al., 2006).

Figure 7. Filled circles mark velocities from borehole logs as a function of resistivity-derived hydrate saturation. Both parameters are averaged over 10 m intervals down the borehole. Lines mark predicted velocities from the SCA/DEM model for a porosity of 38% and a clay content of 57%, which are mean values for the interval studied. Lines are computed for degrees of hydrate cementation of 0%, 25%, 50%, 75% and 100%. a) P wave velocity; b) S wave velocity.

Figure 8. Degree of cementation required to match observed velocities using the modified SCA/DEM model for a variety of datasets. Circles mark the Mallik 2L-38 dataset (Collett et al., 1999); diamonds mark the data of Priest et al. (2005); squares mark the data of Waite et al. (2004); and triangles mark the data of Yun et al. (2005): a) only P wave velocities used b) only S wave velocities used c) degree of hydrate cementation optimised to match both P and S wave velocities, using the misfit function defined by Chand et al. (2006).

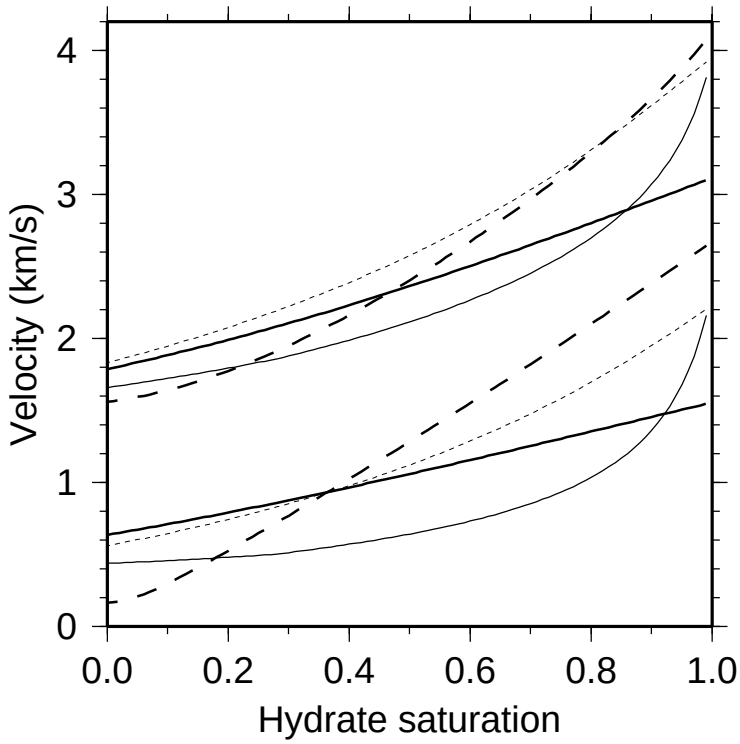

Minshull and Chand Fig. 1

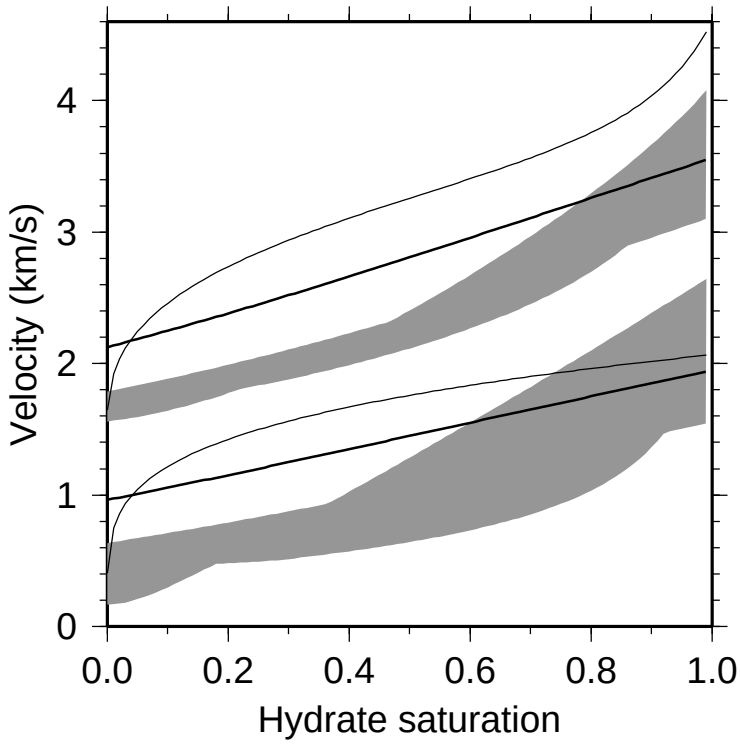

Minshull and Chand Fig. 2

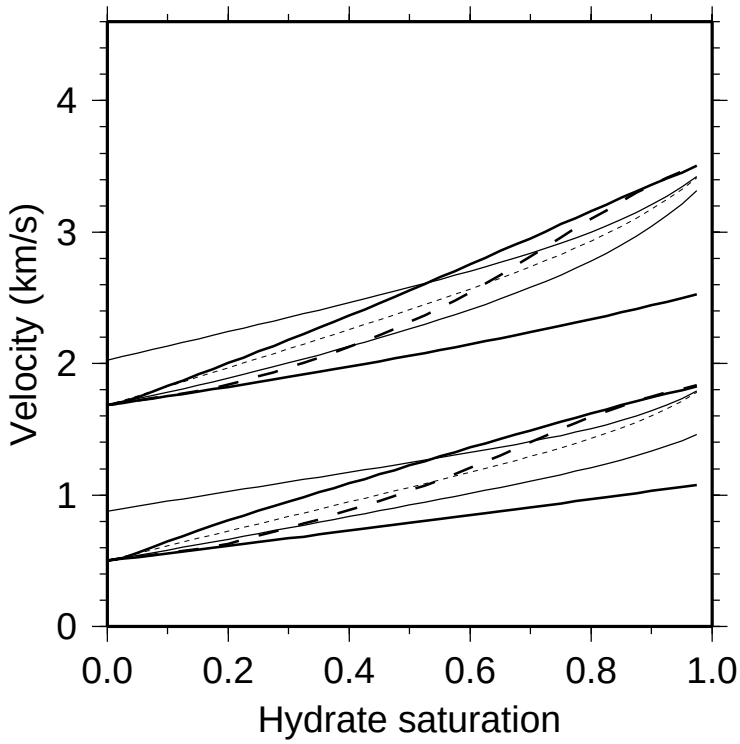

Minshull and Chand Fig. 3

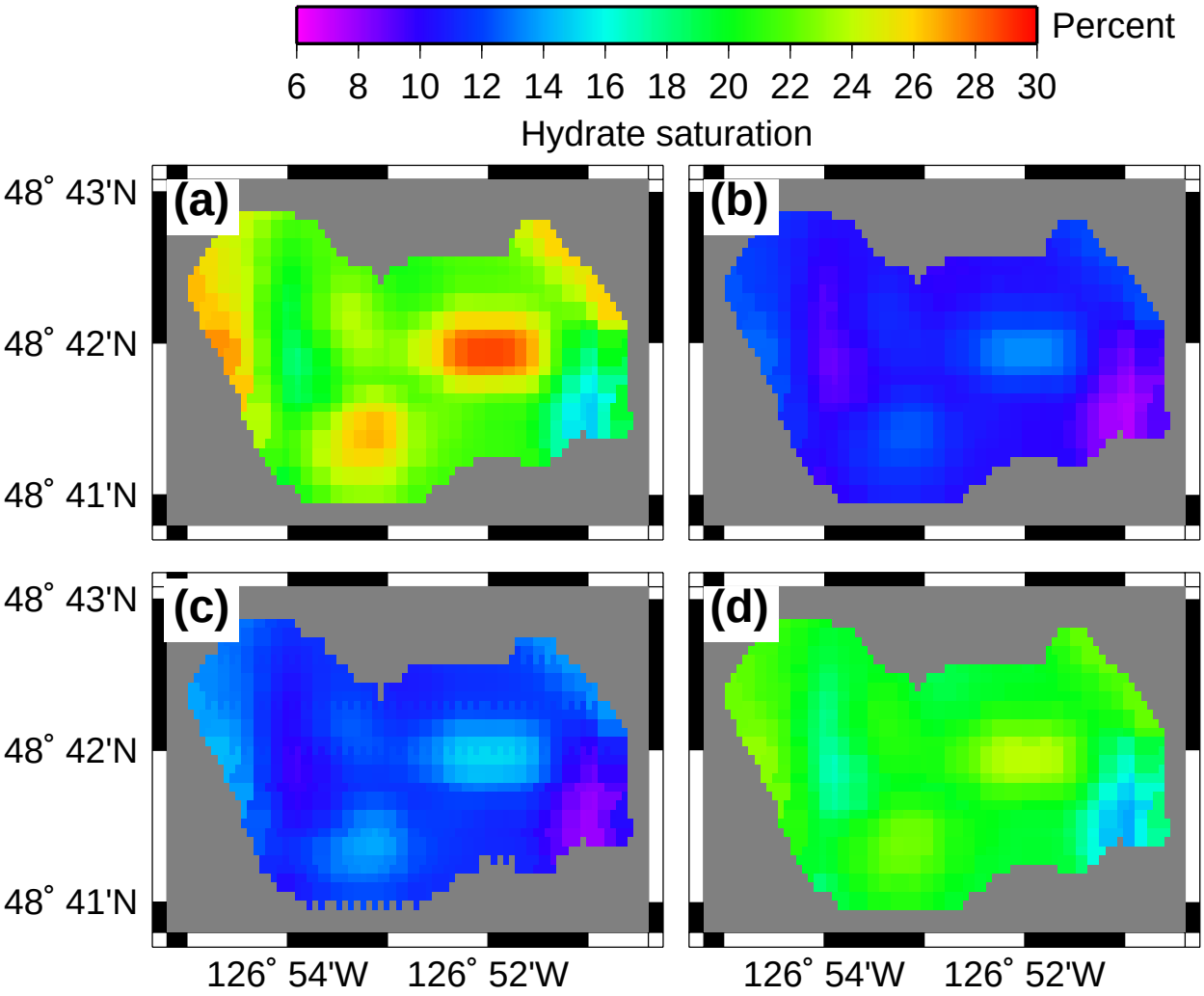

Minshull and Chand Fig. 4

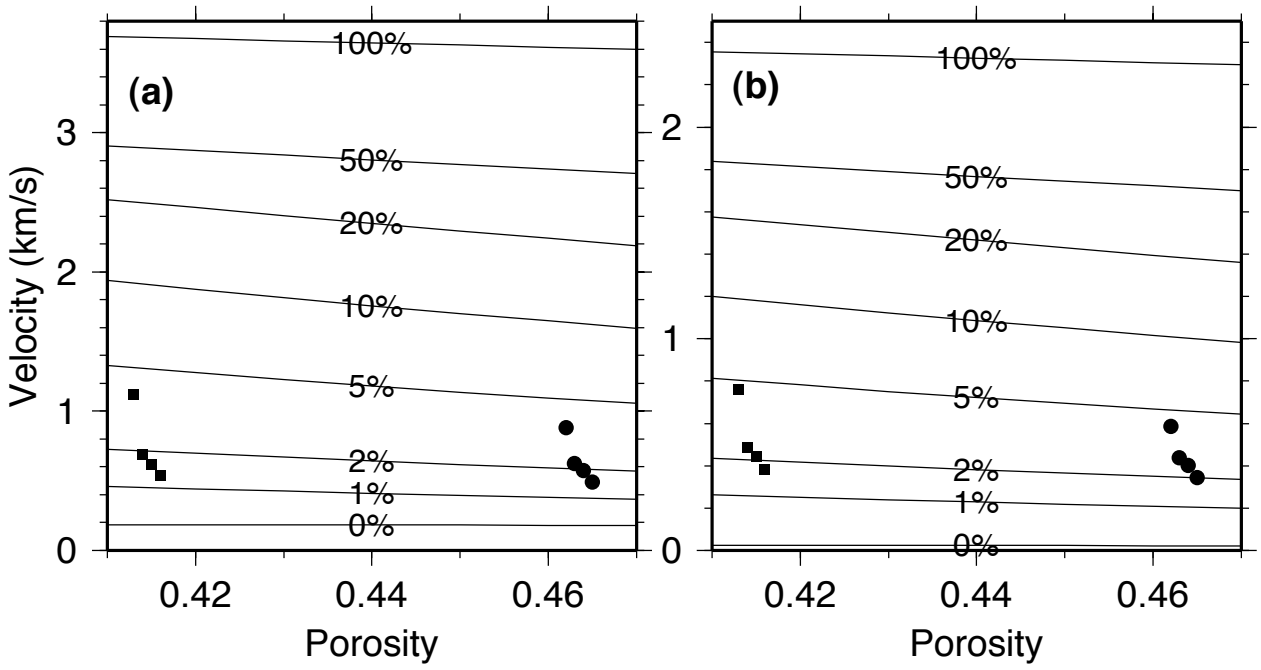

Minshull and Chand Fig. 5

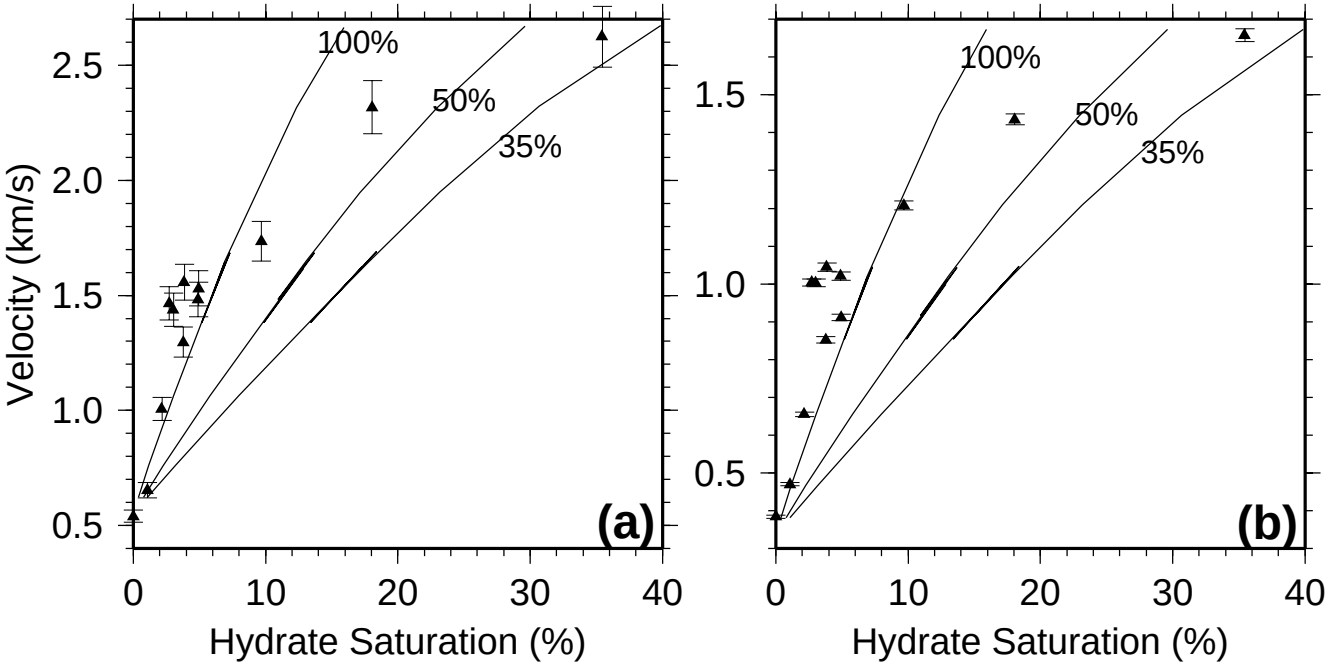

Minshull and Chand Fig. 6

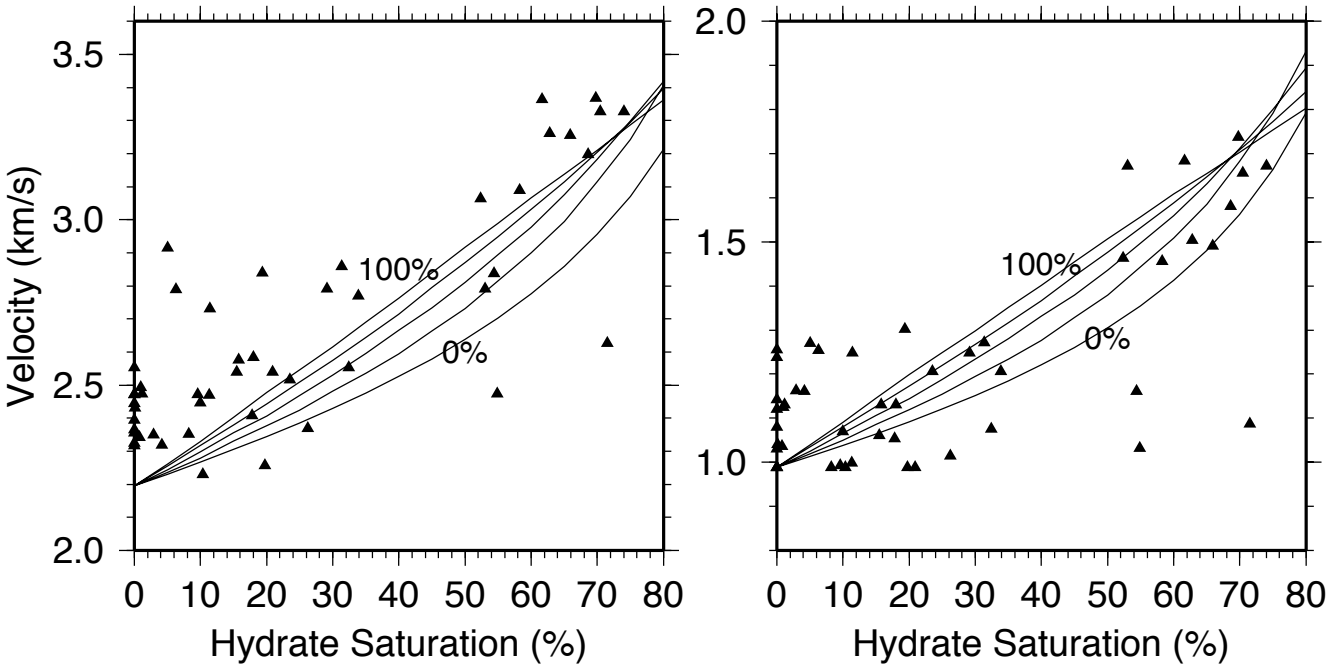

Minshull and Chand Fig. 7

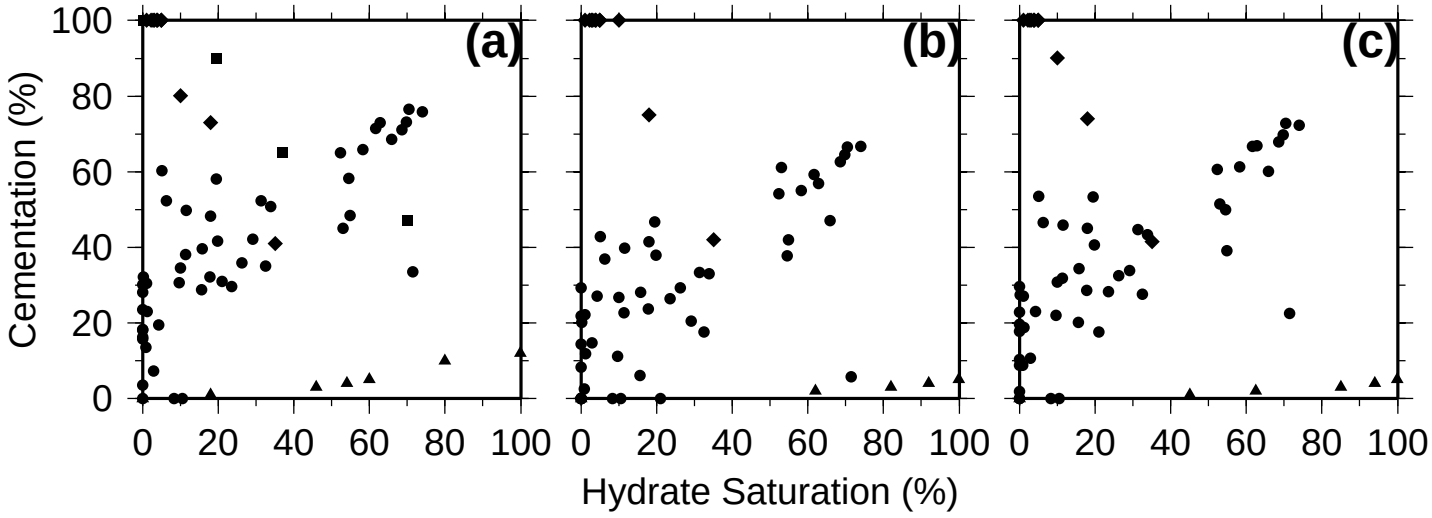

Minshull and Chand Fig. 8